Uniaxial True Stress-Strain after Necking

Yun Ling
AMP Incorporated

ABSTRACT

A weighted-average method for determining uniaxial, true tensile stress vs. strain relation after necking is presented for strip shaped samples. The method requires identification of a lower and an upper bound for the true stress-strain function after necking and expresses the true stress-strain relation as the weighted average of these two bounds. The weight factor is determined iteratively by a finite element model until best agreement between calculated and experimental load-extension curves is achieved. The method was applied to various alloys.

INTRODUCTION

The finite element method (FEM) has become a common engineering tool. If applied to solve mechanical engineering problems it deals mostly with linear elastic problems where the elastic modulus E and Poisson's ratio ν are the only material constants considered. In recent years the demand for nonlinear, plastic analyses has increased noticeably. Crimping results by its very nature in large plastic deformation. It was analyzed recently using FEM by S. Kugener[1]. Another example where plastic behavior of materials must be considered are large deformations of small contacts in high density connectors.

For plastic analysis the FEM requires besides E and ν also input of a uniaxial true stress-strain function. This function is usually determined by the applicable ASTM method[2]. It is well known that in tensile testing, the uniform extension ceases when the tensile load reaches a material specific maximum. At this point the test sample begins to neck. The state of stress changes gradually from the simple uniaxial tension to a complicated condition of triaxial stress for a round bar or of biaxial stress for a thin strip. Because the onset of necking destroys the uniaxial state of stress it is impossible to determine a uniaxial true stress-strain relation by the standard tensile test once necking has started. Thus, for applications in which strain exceeds its value at the onset of necking, the standard tensile test cannot provide data sufficient for modeling. This can seriously limit the use of FEM for large strain applications such as contact forming. For this reason some method has to be found to obtain the true stress-strain relation after necking.

For rods Bridgman's correction method[3] is most commonly used to obtain uniaxial true stress-strain relations after necking. Because electrical contacts are almost exclusively in form of flat bars applicability of the Bridgman correction is rather limited. This extends also to laboratory tests, where samples are required that approach in geometry and dimensions those of the corresponding contacts. To the author's best knowledge, there is no effective way to obtain for strip samples true stress-strain curves after necking. This is a great obstacle for developing a true stress-strain data base for contact spring materials.

The study presented here is an attempt to fill that gap. For reasons of clarity some fundamental definitions and concepts are reviewed and discussed.

FUNDAMENTAL DEFINITION

Strain describes quantitatively the degree of deformation of a body. It is measured most commonly with extensometers and strain gauges. For uniaxial deformation strain can be expressed as

$$e = \frac{L_f - L_0}{L_0}, \qquad (1)$$

where

L_0 = original length of the undeformed specimen,

L_f = length of the deformed specimen.

This strain is the *engineering strain*, or *conventional strain*.

Based on this definition, if a sample were stretched such that $L_f = 2L_0$, the tensile engineering strain would be 100%. On the other hand, if a sample were compressed to the limit such that $L_f = 0$, the compressive engineering strain would again be 100%. These extreme examples show that for large strain the definition of equation (1) is not meaningful.

For purely elastic deformation stresses are uniquely defined by the final configuration of a material, regardless of how this final state is reached. Because of the presence of irreversible elements in the deformation a plastic analysis has to follow the path along which the final configuration is reached. To achieve this, the total deformation is generally divided into small increments. Considering the uniaxial case, let dL be the incremental change in gauge length and L the gauge length at the beginning of that increment. Then, the corresponding strain increment becomes

$$d\epsilon = \frac{dL}{L} \tag{2}$$

and the total strain for a change of the gauge length from L_0 to L_f

$$\epsilon = \int_o^{\epsilon} d\epsilon = \int_{L_0}^{L_f} \frac{dL}{L} = \ln \frac{L_f}{L_0}. \tag{3}$$

The strain defined by equation (3) is the *true strain* or *natural strain*. It is a more suitable definition of strain and is particularly useful for large strain analyses. In the case of a sample being compressed to zero thickness, equation (3) would yield

$$\epsilon_{L_f \to 0} = \lim_{L_f \to 0} \left(\ln \frac{L_f}{L_0} \right) = -\infty$$

which is a more reasonable value than the compressive strain of 100% predicted by definition of equation (1).

True strain and engineering strain are related by

$$\epsilon = \ln (1 + e). \tag{4}$$

A body deforms under an applied load. Expressed as force per unit area of cross section the load becomes a stress, s. For uniform deformation it may be defined as

$$s = \frac{F}{A_o} \tag{5}$$

where

F = force acting perpendicular to the cross section,

A_0 = original cross sectional area.

This stress, defined with reference to the undeformed configuration, is called *engineering stress*. If the reduction of the cross sectional area is large, the engineering stress definition becomes inappropriate. For instance it fails to predict strain hardening simply because of the use of a constant initial area, A_0. A more realistic stress definition should use the instantaneous cross sectional area A:

$$\sigma = \frac{F}{A}. \tag{6}$$

The definition of the stress σ is based on the instantaneous material configuration. It is called the *true stress*. If during a deformation the volume of the sample is conserved, i.e., if

$$AL = A_0F_0 = A_fF_f$$

one may relate true stress and engineering stress by

$$\sigma = s(1 + e). \tag{7}$$

Engineering stress-strain curves are useful only for small deformations. In such cases true stress-strain and engineering stress-strain curves coincide within reasonable limits. For large strain, say greater than 1%, the true stress-strain should always be used. It is important to note that equation (6) holds only for uniform deformation, i.e., where stresses in every point at the cross-section are the same. For the nonuniform case, stress is defined as

$$\sigma = \lim_{\Delta A \to 0} \left(\frac{\Delta F}{\Delta A} \right). \tag{8}$$

Because of the difficulties in measuring independently ΔF and ΔA equation (8), considered solely as a definition, has mostly theoretical value. This implies that the stress σ can be directly obtained only when the deformation is uniform by measuring the force and the corresponding cross sectional area. Once deformation ceases to be uniform, only average stress can be measured and the stress distribution cannot be determined experimentally. This is the main reason for the problems encountered in the attempts to obtain true stress after necking.

UNIAXIAL STATE

In the previous section, stress and strain are defined for the simple uniaxial state of stress. This simplified the introduction of the basic concept of stress and strain without using tensors. More importantly, the uniaxial state of stress is one of the few simple cases in which the stress-strain relation may be verified experimentally.

A general theory of plasticity must deal with states of stress comprising six stress components σ_x, σ_y, σ_z, τ_{xy}, τ_{yz}, τ_{zx} and six strain components ϵ_x, ϵ_y, ϵ_z, γ_{xy}, γ_{yz}, γ_{zx}. Note that here the conventional notations for stresses and strains are used.[4] The uniaxial state of stress is a special case where there is only one

nonzero normal stress

$$\sigma_x = \sigma,$$
$$\sigma_y = \sigma_z = \tau_{xy} = \tau_{yz} = \tau_{zx} = 0. \quad (9)$$

If the material is isotropic, which shall be assumed throughout this paper, the strains in the uniaxial state are:

$$\epsilon_x = \epsilon,$$
$$\epsilon_y = \epsilon_z = -\epsilon/2,$$
$$\gamma_{xy} = \gamma_{yz} = \gamma_{zx} = 0. \quad (10)$$

Note that here, and in the rest of this section, the plastic strains are assumed to be large enough so that the elastic ones can be neglected.

Generally only the stress-strain relation in the uniaxial state is known. Therefore, one needs to relate stresses and strains in a general state to uniaxial observations. For this purpose it is assumed that for any given stress state, there exists an equivalent uniaxial stress state. The equivalent uniaxial stress, or the von Mises, stress is defined as[5]

$$\sigma_e = \frac{1}{\sqrt{2}}\left[\begin{array}{c}(\sigma_x - \sigma_y)^2 + (\sigma_y - \sigma_z)^2 + (\sigma_z - \sigma_x)^2 + \\ + 6(\tau_{xy}^2 + \tau_{yz}^2 + \tau_{zx}^2)\end{array}\right]^{1/2}. \quad (11)$$

The corresponding equivalent strain can be found through

$$\epsilon_e = \int d\epsilon_e, \quad (12)$$

where $d\epsilon_e$ is the strain increment

$$d\epsilon_e = \frac{\sqrt{2}}{3}\left[\begin{array}{c}(d\epsilon_x - d\epsilon_y)^2 + (d\epsilon_y - d\epsilon_z)^2 + (d\epsilon_z - d\epsilon_x)^2 + \\ + 6d\gamma_{xy}^2 + 6d\gamma_{yz}^2 + 6d\gamma_{zx}^2\end{array}\right]^{1/2}. \quad (13)$$

Note that here strain increments are used to account for the possible path-dependent nature of the deformation. The relationship between the equivalent stress σ_e and the equivalent strain ϵ_e follows the measured uniaxial flow curve, i.e.,

$$\sigma_e(\epsilon_e) = \sigma(\epsilon).$$

This can be verified by substituting the uniaxial conditions (9) and (10) into equations (11) and (12), respectively:

$$\sigma_e = \sigma, \qquad \epsilon_e = \int d\epsilon = \epsilon. \quad (14)$$

The general stress-strain relation for plastic deformation may be expressed as

$$d\epsilon_x = \frac{d\epsilon_e}{\sigma(\epsilon_e)}\left[\sigma_x - \frac{(\sigma_y + \sigma_z)}{2}\right], \qquad \text{etc.},$$
$$d\gamma_{xy} = \frac{3}{2}\frac{d\epsilon_e}{\sigma(\epsilon_e)}\tau_{xy}, \qquad \text{etc.}, \quad (15)$$

where $\sigma(\epsilon_e)$, often called the *strain hardening function*, is evaluated from the uniaxial true stress-strain curve.

A special situation occurs when the ratios of the principal stresses remain constant during loading. In this case, the total strains may be related to stresses[5] by

$$\epsilon_x = \frac{\epsilon_e}{\sigma(\epsilon_e)}\left[\sigma_x - \frac{(\sigma_y + \sigma_z)}{2}\right], \qquad \text{etc.},$$
$$\gamma_{xy} = \frac{3}{2}\frac{\epsilon_e}{\sigma(\epsilon_e)}\tau_{xy}, \qquad \text{etc.}, \quad (16)$$

The above discussions show why the uniaxial true stress-strain relation is very important. It defines the strain hardening of a material and determines the general stress-strain relation when plastic deformation is taking place. Thus, measuring the uniaxial true stress/strain relation is the most fundamental task before any plastic analysis can be made. Unfortunately, experimental determination of uniaxial true stress/strain relations by uniaxial tensile test is greatly complicated by the necking phenomenon.

CORRECTION METHOD

In developing a method for finding the true stress/strain relation beyond necking for a round bar, Bridgman assumed[3]

(1) that the strain distribution in the minimum section was uniform with

$$\epsilon_r = \epsilon_t = -\frac{\epsilon_a}{2} \quad (17)$$

where

ϵ_r = radial stress,

ϵ_t = hoop stress,

ϵ_a = axial stress;

(2) that a longitudinal grid line is deformed into a curve at the neck so that, with the quantities identified in Figure 1, its curvature $1/\rho$ is

$$\frac{1}{\rho} = \frac{r}{aR} \quad (18)$$

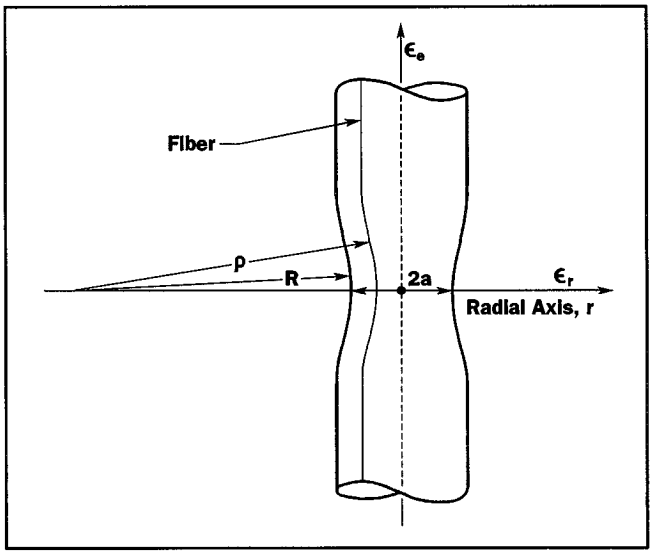

Figure 1. Illustration of necking of a rod and introduction of parameters used in the text.

where

ρ = radius of curvature of the grid line,

r = radius of actual cross section,

a = radius of the smallest cross section,

R = radius of curvature of the neck;

(3) the ratios of the principal stresses remain constant during loading such that the total strain-stress relations (16) may be used.

Based on assumption (1), the equivalent uniaxial strain, ϵ_e, at the minimum section is the average axial strain at the minimum section. Introducing in equation (3) the volume conservation condition and replacing the final cross sectional area, A_f, by the instantaneous minimum cross sectional area, A, it is

$$\epsilon_e = \int_{L_0}^{L_a} d\epsilon_a = \epsilon_a = \ln \frac{A_0}{A}, \tag{19}$$

which means that to obtain the equivalent strain at the neck, one only has to measure the instantaneous dimension of the minimum section.

The average axial or nominal stress, $(\sigma_a)_{av}$, at the smallest cross section is

$$(\sigma_a)_{av} = \frac{F}{A}. \tag{20}$$

Because radial and hoop stresses, σ_r and σ_t, are not zero the nominal stress is not the equivalent uniaxial stress. Using the stress equilibrium equations at the minimum section and the assumptions (2) and (3), Bridgman[3] gives the stress distribution at the smallest cross section as

$$\sigma_r = \sigma_t = \frac{(\sigma_a)_{av}}{\left(1 + \frac{2R}{a}\right)} \left\{ \frac{\ln\left(\frac{a^2 + 2aR - r^2}{2aR}\right)}{\ln\left(1 + \frac{a}{2R}\right)} \right\},$$

$$\sigma_a = \frac{(\sigma_a)_{av}}{\left(1 + \frac{2R}{a}\right)} \left\{ \frac{1 + \ln\left(\frac{a^2 + 2aR - r^2}{2aR}\right)}{\ln\left(1 + \frac{a}{2R}\right)} \right\}. \tag{21}$$

Because the shear stresses disappear at the smallest part of the cross section the equivalent uniaxial stress calculated from equation (11) becomes

$$\sigma_e = \frac{(\sigma_a)_{av}}{\left(1 + \frac{2R}{a}\right) \ln\left(1 + \frac{a}{2R}\right)} = k(\sigma_a)_{av}, \tag{22}$$

with

$$k = \left[\left(1 + \frac{2R}{a}\right) \ln\left(1 + \frac{a}{2R}\right) \right]^{-1},$$

which may be considered as the nominal stress $(\sigma_a)_{av}$ corrected by a factor k.

Verification of this correction method is difficult because true stresses after necking cannot be measured directly but the assumptions on which the correction theory is deserve closer examination. Measurement of strain distributions has shown that they are essentially uniform across the minimum section. Therefore assumption (1) can be considered to be a good approximation.[6] The curvature assumption (2) was verified experimentally by Davidenkov and Spiridonova.[7] Assumption (3) is not fully justified but according to Aronofsky[6] represents a first approximation. Moreover, many finite element analyses, e.g., those by Zhang and Li[8] have shown that stress distribution at the minimum cross section approximately follows equations (21). Therefore, it is generally accepted that if a and R are accurately measured, Bridgman's correction method can predict the true stress-strain relation beyond necking fairly well in a rod. It must be pointed out that for several reasons Bridgman's correction method is not simple to use in practice. It requires a series of tests with different loadings to determine the radius of curvature R and the minimum radius a, which are both difficult to measure with sufficient accuracy.

Based on the same three assumptions Bridgman extended his correction method to flat bars. However, necking for flat samples proved to be much more complicated than for rods with their circular cross section. For thin strips two types of

necking or flow instability must be considered. The first of them is *diffuse necking*, so called because its extent is much greater than the sample thickness. It is illustrated in Figure 2. This form of instability is analogous to necking of rods. Diffuse necking starts when the tensile load reaches its maximum. It may terminate in fracture but is often followed by a second instability process called *localized necking* of thin strips. In this mode the neck is a narrow band inclined at an angle to the specimen axis, as shown in Figure 2. Once localized necking started, the width of the sample contracts little, but the thickness along the necking band shrinks rapidly. Fracture occurs soon after.

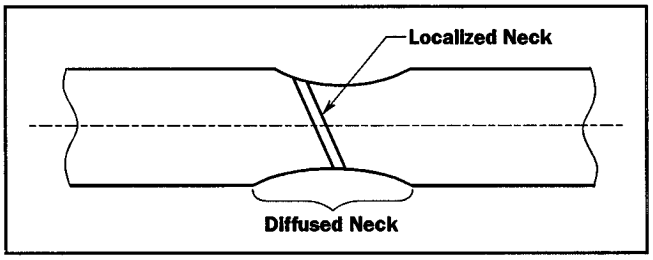

Figure 2. Illustration of the difference between localized and diffused neck during necking of a thin strip.

Bridgman's correction method for flat samples does not consider localized necking. Therefore, it is not surprising that the method apparently has not been applied successfully. The reason for the failure is that all three assumptions were found to be incorrect for flat strips:

- The strain distribution at the minimum cross-section becomes highly non-uniform when localized necking begins. The average axial strain

$$(\epsilon_x)_{av} = \ln\left(\frac{A_0}{A}\right), \qquad (23)$$

  can be considerably smaller than the maximum axial strain at the minimum cross section.[6] Thus, even if the instantaneous dimension of the minimum section is known, the equivalent strain is still not defined. More complicated techniques such as the grid method have to be used to measure strain across the minimum cross section.
- To obtain the equivalent uniaxial stress, one has to solve for the distribution of stresses σ_x and σ_y across the minimum section. To do this analytically, one needs to find the curvatures of the longitudinal grid lines during necking. Aronofsky's experimental work[6] suggests that Bridgman's curvature assumption does not apply to flat samples. One would have to measure the curvature not only for the outer profile but also for many other longitudinal grid lines across the minimum section. This would make the testing difficult and time consuming.
- The ratios of the principal stresses do not remain constant during loading and the incremental theory of plasticity may have to be used, which makes the analytical solution for the stress distribution at the minimum section very difficult, if not impossible.

Although theoretically development of a correction method for obtaining the true stress/train relation after necking for flat samples is still possible, it would be very difficult and costly to apply it.

WEIGHTED AVERAGE METHOD

Correction methods were developed before the powerful FEMs were available. FEM was shown to permit simulation of the necking phenomenon very well. There have been numerous studies on this subject.[9] Most of them focused on the problem of how necking develops for a given stress-strain relation. The opposite, practically more important problem, of finding for a given load-extension curve the corresponding true stress-strain function attracted little attention.

The only such work the present author is aware of is by Zhang and Li.[8] There, the experimental tensile load-extension curve is considered as target and the true stress-true strain relation is searched for iteratively by finite element analysis (FEA) until the target is reached within a certain tolerance. The method worked well for a round sample of a middle-carbon steel: the obtained true stress-strain relation was in good agreement with that determined by Bridgman's correction method. Though Zhang and Li studied only round samples, the concept applies also to flat samples. The main advantage of their method is that the true stress-true strain data can be extracted from results of standard tensile tests which does not have to be interrupted at different loads to determine profiles and dimensions at the neck, as required by the correction method. The main shortcoming is that the entire stress-strain relation beyond necking is treated as unknown and iterations are required for a series of strain intervals making the computation extremely extensive and time-consuming. Another drawback is that the method requires a specially written FEA program to do the numerical searching. For most engineers, developing a robust FEA program for nonlinear plastic analysis is not a trivial task. Therefore, availability of a method similar in principle to Zhang and Li's approach but much simpler is highly desirable.

A power law is often used to represent the whole flow curve[10], for instance

$$\sigma = K\epsilon^n, \qquad (24)$$

where K and n are empirical constants determined from known true stress-strain data before necking. Modern FEA programs do not require input of the uniaxial true stress-strain function in analytical form. It is entered numerically as ordered pairs taken from experimental data and the power law or any other function in analytical form are not necessary for curve fitting the measured true stress-strain data before necking. The power law may be useful for extrapolation of the true stress-strain curve beyond necking.

Let ϵ_u be the true strain at which necking starts and σ_u the

corresponding true stress. They can be calculated from the ultimate tensile strength s_u and the corresponding uniform engineering strain e_u:

$$\epsilon_u = \ln(1 + e_u),$$
$$\sigma_u = s_u(1 + e_u). \tag{25}$$

At the onset of necking it is

$$\sigma\big|_{\epsilon=\epsilon_u} = \sigma_u,$$

and

$$\left.\frac{d\sigma}{d\epsilon}\right|_{\epsilon=\epsilon_u} = \sigma_u. \tag{26}$$

Note that the second equation in (26) is the well known condition for initial necking. If the power law is used to extrapolate the true stress-strain relation beyond necking, the onset of necking should be reserved, i.e., the constants K and n are determined by equations (26) as

$$K = \frac{\sigma_u}{\epsilon_u^{\epsilon_u}}$$

and

$$n = \epsilon_u$$

and the extrapolation equation becomes

$$\sigma = \left(\frac{\sigma_u}{\epsilon_u^{\epsilon_u}}\right)\epsilon^{\epsilon_u}. \tag{27}$$

In a log-log plot the power-law is represented by a straight line. However, from observation it is known that in a log-log diagram of the true stress vs. true strain curve the slope tends to increase slightly beyond necking. This behavior is illustrated in Figure 3 for a phosphor bronze alloy. It was observed for all copper alloys examined, which included phosphor bronze, brass, pure copper, and beryllium copper. Thus, the power-law extrapolation appears to underestimate true stresses and it is reasonable to assume that for copper alloys the power law extrapolation gives a lower bound for the true stress.

For many copper alloys, a straight line was found to represent the true stress-strain relation better than the power law. Thus, one may also assume a linear relationship between the true stress and true strain after necking

$$\sigma = a_0 + a_1\epsilon, \tag{28}$$

where a_0 and a_1 are two constants, determined from equations (26) as $a_0 = \sigma_u(1\text{-}\epsilon_u)$ and $a_1 = \sigma_u$, which yields

$$\sigma = \sigma_u(1 + \epsilon - \epsilon_u). \tag{29}$$

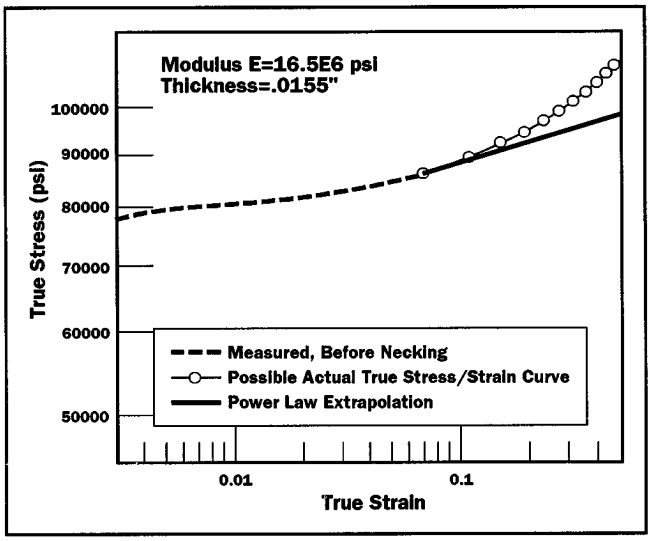

Figure 3. True stress-strain plot. The log-log presentation shows that the power law extrapolation tends to underestimate the true stress.—Sample: C511-Hard-Longitudinal. For additional data see Table 1.

The linear extrapolation suggests that after necking the slope $d\sigma/d\epsilon$ of the true stress-true strain curve remains constant, or the strain hardening rate does not change as the strain becomes large. Observation shows that this is usually not the case: strain hardening rate generally decreases with increasing true strain. Therefore, the linear extrapolation will generally lead to overestimate true stresses and give an upper bound.

Since the lower and upper bounds for true stresses after necking have been identified, a better approximation of the true stress is to use the weighted average of the lower and upper bounds defined by equations (27) and (29), respectively:

$$\sigma = \sigma_u\left[w(1 + \epsilon - \epsilon_u) + (1 - w)\left(\frac{\epsilon^{\epsilon_u}}{\epsilon_u^{\epsilon_u}}\right)\right], \tag{30}$$

where w, with $0 \le w \le 1$ is an unknown weight constant. The upper boundary of this closed interval, i.e., $w = 1$ represents the linear extrapolation, the lower bound, $w = 0$, the power law. The central point, $w = 1/2$, is the average of both.

To determine the weight constant w Zhang and Li's approach[8] is followed. The measured tensile load-extension relation, F(e), i.e., the engineering curve is considered the target and the weight constant w is varied in a finite element model until the calculated load-extension relation $F^*(e,w)$ agrees with F(e) within pre-defined limits. This optimization problem can be formulated as

$$\min_{0\le w\le 1}(\delta), \tag{31}$$

where δ is an error measuring the difference between $F^*(e,w)$

and F(e), for instance

$$\delta = \int_{e_u}^{e_f} [F^*(e, w) - F(e)]^2 \, de \qquad (32)$$

with e_f = relative elongation, or engineering strain, immediately prior to fracture. Note that the error is evaluated from the onset of necking to fracture, since the true stress-strain relation before necking has been well defined and the load-extension relation can be measured precisely before necking.

The weighted average method presented in this paper uses only one variable w, while in Zhang and Li's method the searching has to be done for a series of stresses and strains. It is thus a far simpler method. Moreover, it was found experimentally that the largest error always occurs immediately before fracture, i.e., at $e = e_f$. When $F^*(e_f,w) \approx F(e_f)$, the calculated load-extension curve matches the experimental one very well. Thus, instead of performing the rigorous optimization process, one may simply determine w such that

$$\frac{F^*(e_f, w)}{F(e_f)} - 1 \approx 0. \qquad (33)$$

Usually a satisfactory value of w can be obtained by a few trials. Examples are given below.

RESULTS

The finite element program ABAQUS[11] was used to simulate the tensile test. One fourth of the sample was modeled, as shown in Figure 4, using the eight-node-plane-stress element with reduced integration (CPS8R). Necking is induced by the end condition and generally no imperfection in width is needed to initiate it. Fine meshing is located near the center of the sample where the strain gradient is expected to be large. Models with meshes of 20 by 8 and 25 by 10 within the gauge length are analyzed to check numerical convergence. The load-extension curves obtained for the two different meshes were found to be almost identical. Thus, the mesh of 20 by 8 was considered adequate.

The materials of the examples are listed in Table 1. They include various copper alloys of various tempers ranging from very soft pure copper (C10200-1/8Hd) to high temper phosphor bronze (C52100-10M). For phosphor bronze C51100, a weighting constant w = 0.50 was tried first. The corresponding load-extension, i.e., the engineering stress-strain curve is shown in Figure 5a. The calculated curve is slightly below the measured one, indicating that using w = 0.50 slightly underestimates actual strain hardening. Thus, a slightly larger value w = 0.55 was tried with the result that calculated and experimental load-extension curves agreed well. Further refinement led to a value of w = 0.54, which yielded almost perfect agreement. The resulting true stress-strain relation is shown in Figure 5b. For other materials listed in Table 1 experimental load-extension curves and the resulting true stress-strain relations are shown in Figures 6 to 9.

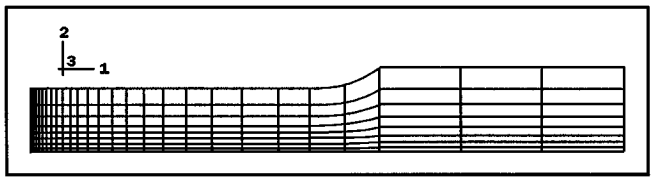

Figure 4. Finite element mesh.

All examples show that the target load-extension curve can be reproduced by simulation with great accuracy provided the true stress-strain relation after necking is adjusted by choosing a proper weight constant w. The question if the true stress-strain relation found by this method is the correct one in an absolute sense remains open. A rigorous proof would have to consider the issue of the uniqueness of the solution. Instead of attempting such proof an engineering argument is offered here. When true stresses are underestimated, a material possesses less strain hardening than it should have. This insufficient strain hardening is directly reflected in the calculated load-extension curve, which would fall below the experimentally determined target curve. Consequently, it will predict that necking develops too fast or too early after its initiation. On the other hand, if true stresses are overestimated, the material will have excessive strain hardening, and the calculated load-extension curve will be above the target curve, which means that necking would develop too slowly or too late. Therefore, a true stress-strain relation that reproduces the experimentally determined load-extension curve should correctly represent the strain hardening function of a material.

To further verify the weighted-average method, a rod of a mild carbon steel is considered. Tensile test data for this material have been reported by Zhang and Li.[8] They also measured the nominal stress and applied Bridgman's correction method to obtain the uniaxial true stress-strain function up to fracture. The

Table 1. Mechanical properties of alloys studied. L = longitudinal, T = transverse.

Alloy	Temper	Orientation	Modulus E, Mpsi	Tensile Strength s_u, kpsi	Uniform Strain e_u, %	Elongation e_f, %	Sample Thickness t, mils
C51100	Hd	L	16.5	80.6	7.60	11.0	15.5
C52100	10M	L	15.6	120.7	1.87	7.20	13.9
C26000	Extra Hd	L	15.5	84.4	4.38	9.60	12.6
C10200	1/8 Hd	T	16	35	30.5	42.0	45.5
C17510	TM04	T	18	124.1	11.0	14.4	8

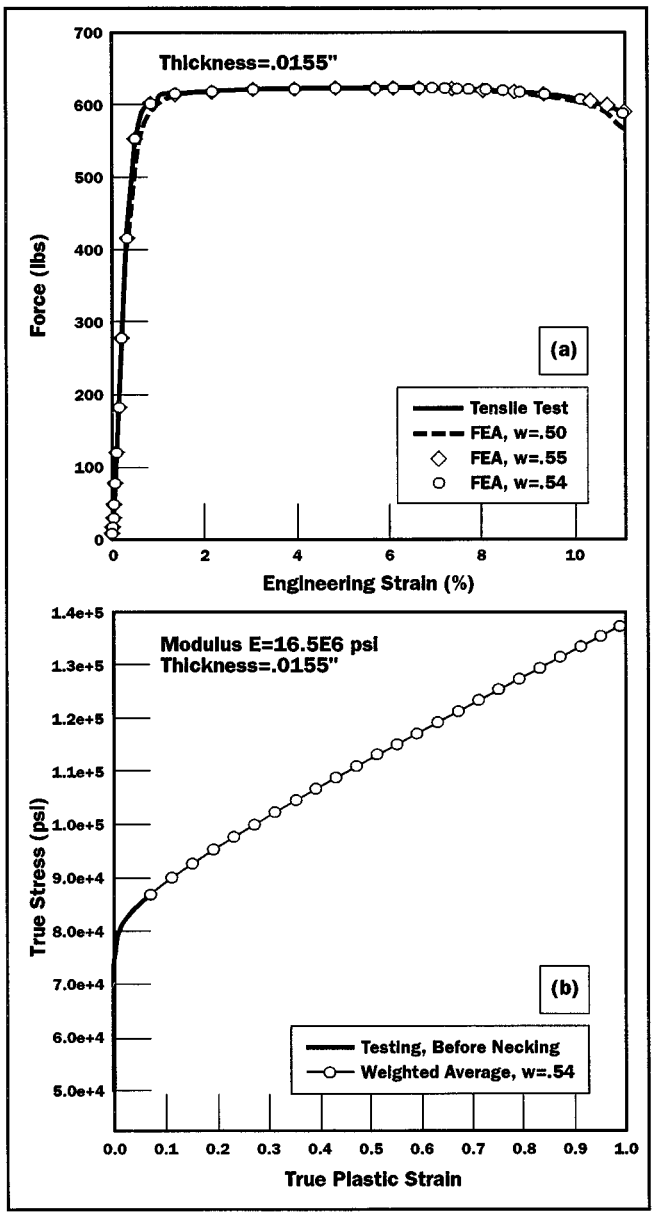

Figure 5. Comparison of load vs. engineering strain with true stress vs. strain for alloy C51100. (a) Load vs. engineering strain curves. (b) True stress vs. true plastic strain curve.—Sample: C511-Hard-Longitudinal.

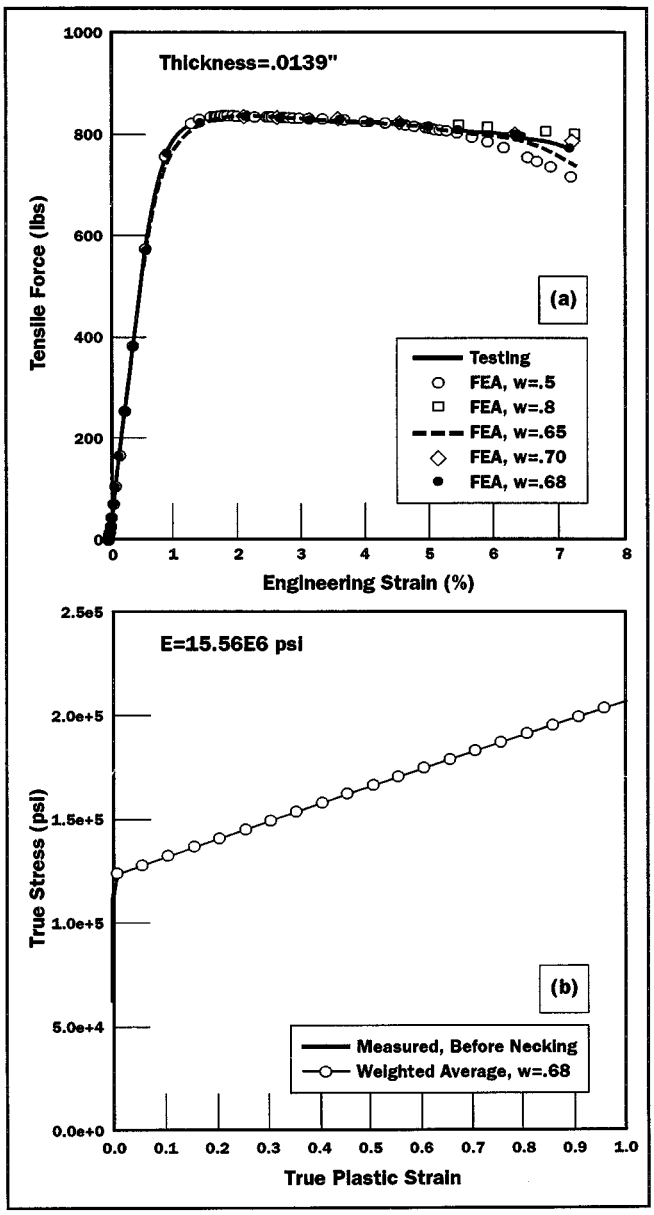

Figure 6. Comparison of load vs. engineering strain with true stress vs. strain for alloy C521. (a) Load vs. engineering strain curves; applied weight constants, w, used for FEA are given in the insert. (b) True stress vs. true plastic strain curve.—Sample: C521-10 M-Longitudinal.

purpose here is to check whether the true stress-strain relation determined by the weighted-average method agrees with that obtained by Bridgman's correction method. By simulating the tensile test of the rod with different weight constants w, it was found that with a weight constant of about 0.45 the calculated load-extension curve agrees well with the experimental one. The results are shown in Figure 10. In Figure 11 are compared the true stress-strain relation after necking calculated by equation (30) with $w = 0.45$, the true stress-strain data determined by Bridgman's correction method and those found by the Zhang and Li procedure. The results from the three methods are quite close. It is concluded that the weighted-average method predicts the true stress-strain relation after necking as well as the two other methods. The results also show that all calculated weight constants are in the range $0 \leq w \leq 1$. This verifies the lower and upper bound assumption at least for the materials studied.

Not yet addressed was the question of how to predict the end of the true stress-strain curve, i.e. the prediction of the fracture strain. To solve this problem one needs to follow the strain

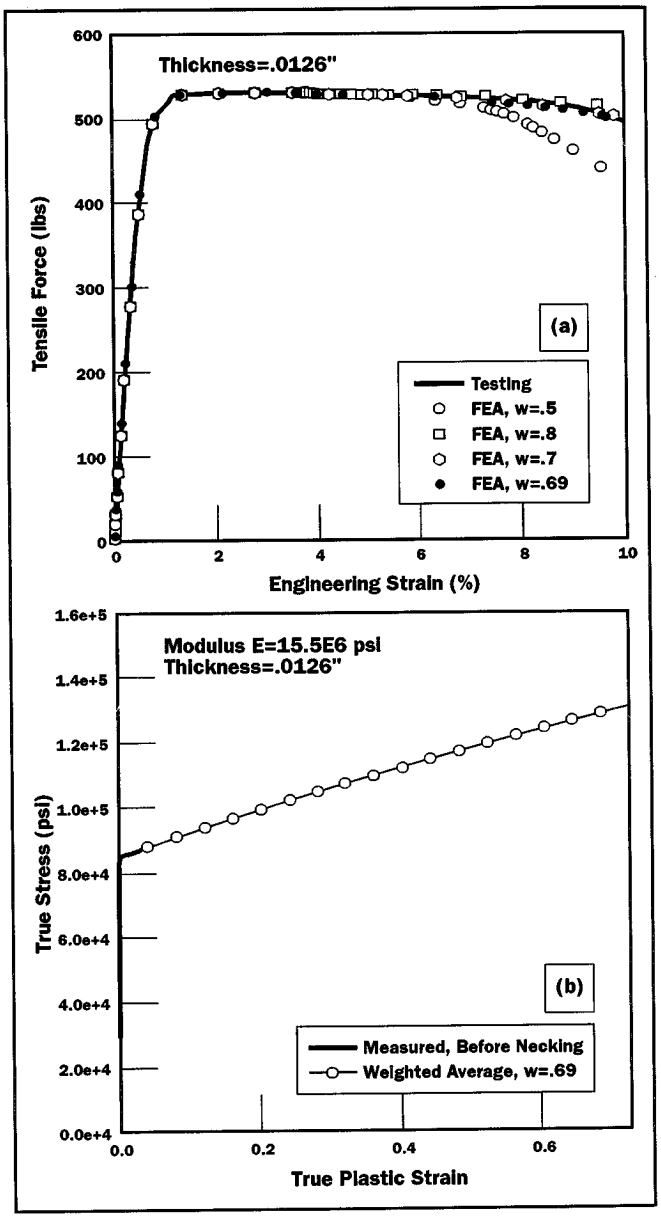

Figure 7. Comparison of load vs. engineering strain with true stress vs. strain for alloy C26000. (a) Load vs. engineering strain curves; applied weight constants, w, used for FEA are given in the insert. (b) True stress vs. true plastic strain curve.—Sample: C260-Extra Hd-Longitudinal.

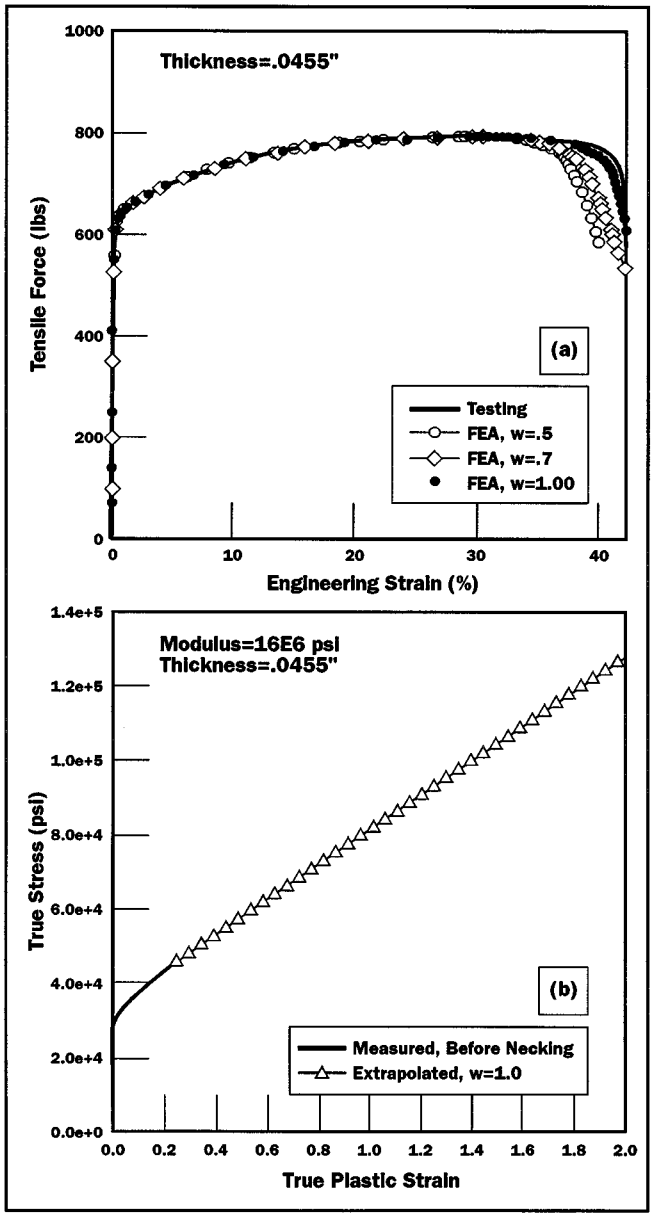

Figure 8. Comparison of load vs. engineering strain with true stress vs. strain for alloy C10200. (a) Load vs. engineering strain curves; applied weight constants, w, used for FEA are given in the insert. (b) True stress vs. true plastic strain curve.—Sample: C102-1/8 Hd-Transverse.

evolution during tensile loading. It is known that fracture in a tensile sample occurs first at the center of the sample because the maximum strain occurs there. For phosphor bronze C51100 it is shown in Figure 12 the maximum strain evolution with increasing engineering strain. The strain in the axial direction is referred to as the major strain, that in the width direction as the minor strain. The equivalent strain is almost the same as the major strain. Since the elongation e_f is the maximum engineering strain the sample can withstand without failure, the equivalent strain corresponding to the elongation should be the fracture strain ϵ_f. It can be found from Figure 12 to be $\epsilon_f \approx 98\%$. The results of calculations of strain values at fracture for various alloys are summarized in Table 2.

It should be pointed out that though the weighted-average method in theory can be used to determine fracture strain, a close look at Figure 12, however, suggests that it is unlikely to yield reliable results. As mentioned before, thin flat samples generally fracture during localized necking. Once this mode has started, the strain increases very rapidly. This can be seen from

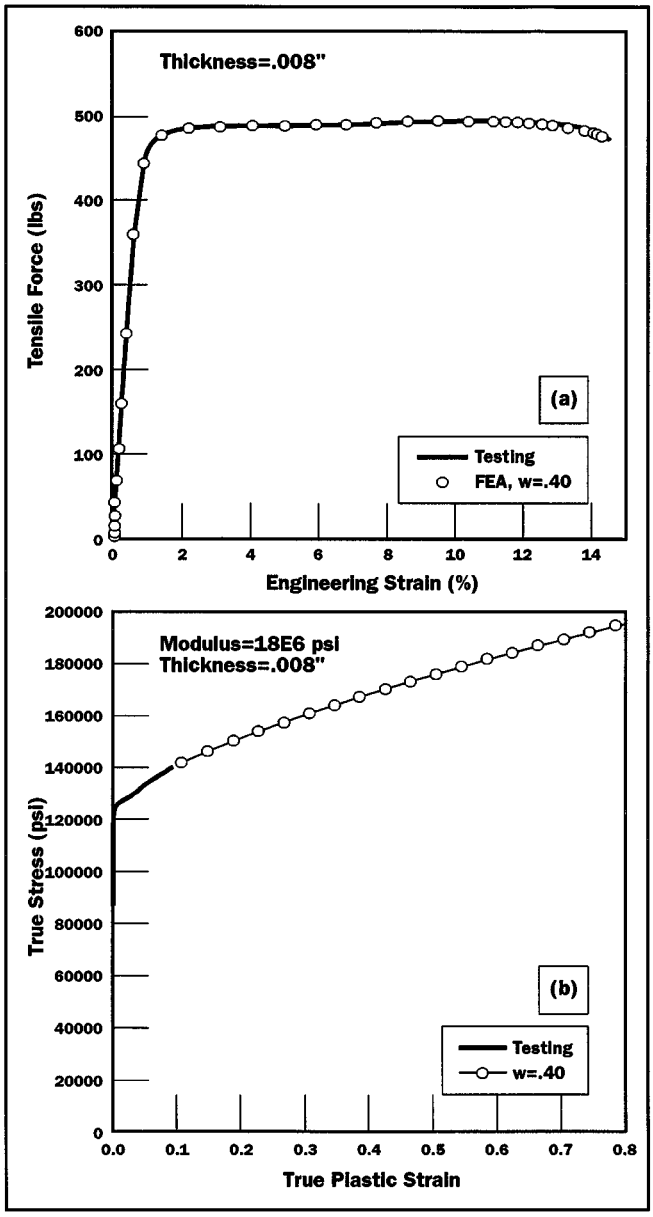

Figure 9. Comparison of load vs. engineering strain with true stress vs. strain for alloy C17510. (a) Load vs. engineering strain curves; applied weight constant, w, used for FEA is given in the insert. (b) True stress vs. true plastic strain curve.—Sample: C17510-TM04-Transverse.

Figure 12 where it is shown that the maximum strain increases very steeply near fracture. Calculations involving such large slopes are usually not reliable. A slight variation in elongation or even a small numerical disturbance can cause significant differences in the calculated fracture strain. The large slope of experimental load-deflection curves near fracture also makes accurate measurements of fracture strain very difficult. In fact, fracture strains determined in formability testing generally have a great deal of scattering.[12] Thus, it is unlikely that one can accurately determine the fracture strain through calculation or

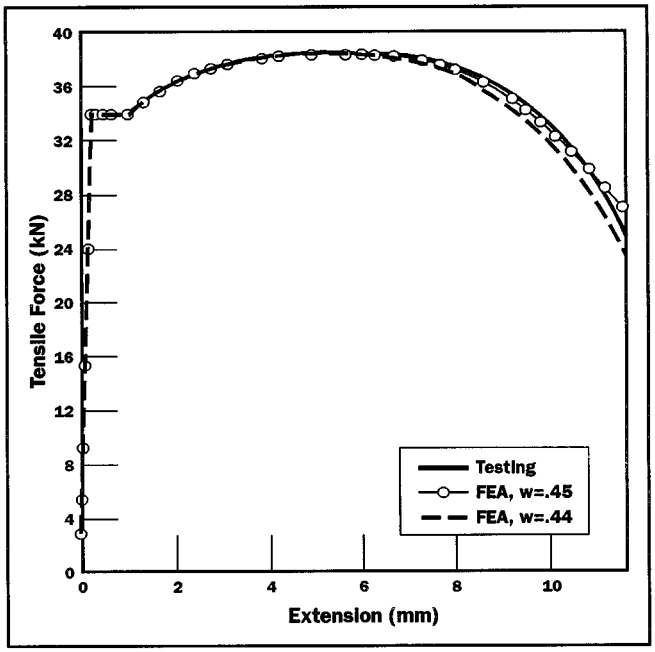

Figure 10. Comparison of calculated and measured load vs. extension curves. Measured data according to Zhang and Li[8].

even through conventional or standardized measurement techniques. At best a conservative estimate of the fracture strain can be given. One way to do this is to measure the cross sectional area A_f at fracture and use the average axial strain in the small-

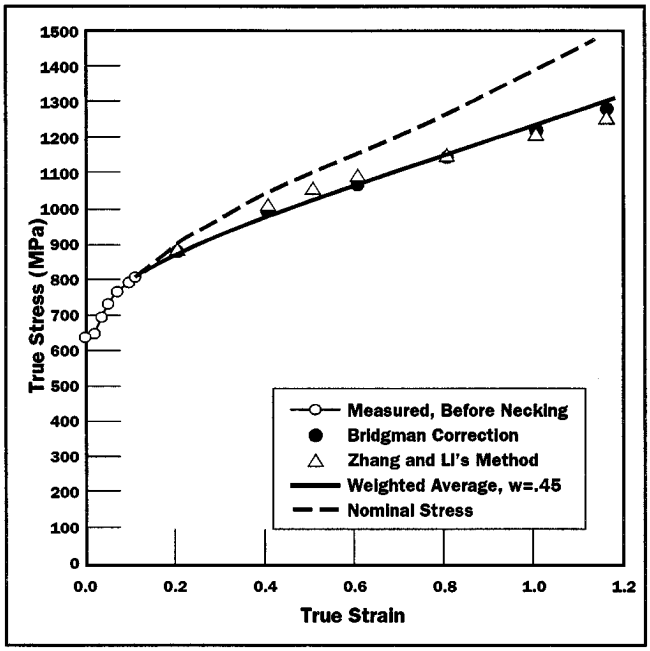

Figure 11. Comparison of true stress vs. strain relationships obtained by different methods. Measured data according to Zhang and Li[8].

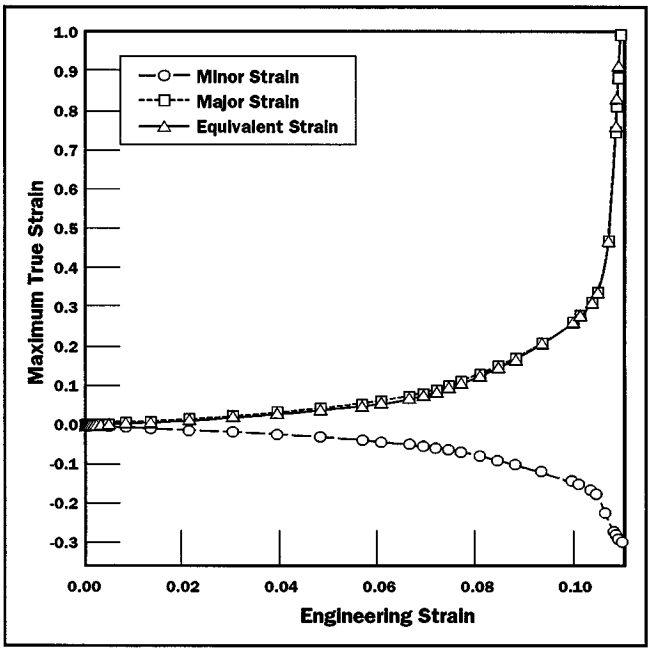

Figure 12. Illustration of changes of maximum true strain with increasing values of engineering strain.—Sample: C511-Hard-Longitudinal.

est section

$$\epsilon_f = \ln\left(\frac{A_0}{A_f}\right) \tag{34}$$

as the fracture strain. This method will yield a conservative estimate because the maximum strain at this section can be considerably larger. Estimation of ϵ_f using this approach is essentially the same as that for rods and has been applied frequently.[13]

CONCLUSION

A new method for predicting true stress-strain functions from engineering stress-strain data was developed and shown to offer advantages over methods commonly known. The new method utilizes weighted averages of upper and lower bound of stress-strain curves and is consequently called the *weighted average method*. Bridgman's correction method is shown to be inappropriate for determining true stress-strain functions for strip samples after necking.

The power law extrapolation of the true stress-strain relation beyond necking is found, at least for the materials listed in Table 1, to be the lower bound for the true stress-strain relation, a linear extrapolation with properly determined constants serves as the upper bound. Using a weight constant, w, the actual true stress-strain function after the onset of necking can be well represented by the weighted average of the two bounds

$$\sigma = \sigma_u \left[w(1 + \epsilon - \epsilon_u) + (1 - w)\left(\frac{\epsilon^{\epsilon_u}}{\epsilon_u^{\epsilon_u}}\right)\right], \tag{35}$$

$$\text{with } 0 \le w \le 1.$$

This expression is suitable for reproducing experimental tensile load-extension curves in FEA with great accuracy by proper selection of the weight constant w.

The weighted average method is not recommended for prediction of fracture strain. Instead, the conventional method involving measuring the minimum cross-sectional area at fracture may be used.

Table 2. Calculated strains values at fracture.

Alloy	Temper	Orientation	Weight constant w	Major Strain, %	Minor Strain, %	Equivalent Strain, %
C51100	Hd	L	0.54	98	−28	98
C52100	10M	L	0.68	92	−26	94
C26000	Extra Hd	L	0.69	70	−26	72
C10200	1/8 Hd	T	1.00	216	−50	220
C17510	TM04	T	0.40	76	−28	76

REFERENCES

1. S. Kugener, ''Simulation of the Crimping Process by Implicit and Explicit Finite Element Methods,'' AMP J. of Technol., **4**, 8-15 (1995).

2. ASTM E 8M—86a, ''Tensile Testing of Metallic Materials,'' *Annual Book of ASTM Standards*, **03.01** (ASTM, Philadelphia, PA, 1987).

3. P.W. Bridgman, *Studies in Large Plastic Flow and Fracture* (McGraw-Hill, New York, 1952).

4. G.E. Dieter, *Mechanical Metallurgy* (McGraw-Hill, New York, 1986).

5. R. Hill, *The Mathematical Theory of Plasticity* (Clarendon, Oxford, 1950).

6. J. Aronofsky, ''Evaluation of Stress Distribution in the Symmetrical Neck of Flat Tensile Bars,'' J. App. Mech., **March 1951**, 75-84 (1951).

7. N.N. Davidenkov and N.I. Spiridonova, ''Analysis of the State of Stress in the Neck of a Tensile Test Specimen,'' Proc. ASTM, **46**, 1147-1158 (1946).

8. K.S. Zhang and Z.H. Li, ''Numerical Analysis of the Stress-Strain Curve and Fracture Initiation for Ductile Material,'' Engrng. Fracture Mech., **49**, 235-241 (1994).

9. V. Tvergaard, ''Necking in Tensile Bars with Rectangular Cross-Section,'' Comp. Meth. Appl. Mech. and Engrng., **103**, 273-290 (1993).

10. J.H. Hollomon, ‘‘Tensile Deformation,’’ Trans. AIME, **162**, 268 (1945).

11. ABAQUS/STANDARD User’s Manuals, Version 5.4, (Hibbitt, Karlsson & Sorensen, Inc., Pawtuckett, RI, 1994)

12. A.A. Tseng, ‘‘Material Characterization and Finite Element Simulation for Forming Miniature Metal Parts,’’ Finite Elements in Analysis and Design, **6**, 251-265 (1990).

13. W.F. Hosford and R.M. Caddell, *Metal Forming: Mechanics and Metallurgy* (PTR Prentice Hall, Englewood Cliffs, NJ, 1993).

Yun Ling is a Senior Development Engineer in the Global Technology Group of AMP Incorporated, Harrisburg, Pennsylvania.

Dr. Ling received his Bachelor of Science and Master of Science degrees in mechanical engineering from Nanjing Institute of Technology, China, and earned a Ph.D. degree in mechanical engineering from the State University of New York at Binghamton. He published more than 15 technical papers in the fields of rotor dynamics, hyperelasticity, materials characterization, and electronic packaging. His present interest is focussed on mechanical properties of materials and connector mechanics.